A CellAge epigenetic clock for expedited discovery of anti-ageing compounds *in vitro*

Celia Lujan[1,*], Eleanor J. Tyler[2,*], Amy P. Webster[3,*], Eleanor R. Stead[1], Victoria E. Martinez Miguel[1], Simone Ecker[3], Deborah Milligan[2], James C. Garbe[4], Martha R. Stampfer[4], Stephan Beck[3,#], Robert Lowe[5,#], Cleo L. Bishop[2,#], Ivana Bjedov[1,#]

Affiliations

[1]: UCL Cancer Institute, Paul O'Gorman Building, University College London, 72 Huntley Street London, London WC1E 6DD, UK
[2]: Centre for Cell Biology and Cutaneous Research, Blizard Institute, Barts and The London School of Medicine and Dentistry, Queen Mary University of London, 4 Newark Street, London E1 2AT
[3]: Medical Genomics Group, UCL Cancer Institute, University College London, London WC1E 6BT, UK
[4]: Biological Systems and Engineering Division, Lawrence Berkeley National Laboratory, Berkeley, CA, United States
[5]: Centre for Genomics and Child Health, Blizard Institute, Barts and The London School of Medicine and Dentistry, Queen Mary University of London, 4 Newark Street, London E1 2AT

*Equal contribution
#corresponding authors :
i.bjedov@ucl.ac.uk c.l.bishop@qmul.ac.uk rlowe.compbio@gmail.com s.beck@ucl.ac.uk

Abstract

We aim to improve anti-ageing drug discovery, currently achieved through laborious and lengthy longevity analysis. Recent studies demonstrated that the most accurate molecular method to measure human age is based on CpG methylation profiles, as exemplified by several epigenetics clocks that can accurately predict an individual's age. Here, we developed CellAge, a new epigenetic clock that measures subtle ageing changes in primary human cells *in vitro*. As such, it provides a unique tool to measure the effects of relatively short pharmacological treatments on ageing. We validated our CellAge clock against known longevity drugs such as rapamycin and trametinib. Moreover, we uncovered novel anti-ageing drugs, torin2 and Dactolisib (BEZ-235), demonstrating the value of our approach as a screening and discovery platform for anti-ageing strategies. CellAge outperforms other epigenetic clocks in measuring subtle ageing changes in primary human cells in culture. The tested drug treatments reduced senescence and other ageing markers, further consolidating our approach as a screening platform. Finally, we showed that the novel anti-ageing drugs we uncovered *in vitro,* indeed increased longevity *in vivo*. Our method expands the scope of CpG methylation profiling from measuring human chronological and biological age from human samples in years, to accurately and rapidly detecting anti-ageing potential of drugs using human cells *in vitro*, providing a novel accelerated discovery platform to test sought after geroprotectors.

One of the remarkable achievements of developed countries is a continuous increase in life expectancy at birth, leading to greater longevity. However, a higher proportion of elderly in modern societies is accompanied by a steep increase in people suffering from age-related diseases. For example, cancer incidence rates, currently at 17 million worldwide, are expected to increase to 26 million in 2040[1], and a similar rise is expected for Alzheimer's and Parkinson's disease[2]. Compression of late-life morbidity is, therefore, a priority to alleviate suffering in the elderly[3] and to reduce a growing economic burden to society[4].

Critically, seminal discoveries in the biology of ageing showed that ageing is a malleable process and that down-regulation of major cellular nutrient signalling pathways, either glucose-sensing insulin signalling or amino acid-sensing target-of-rapamycin signalling, results in longevity and health improvement in all model organisms tested from yeast to mammals[5]. For instance, the long-lived mutants in *C. elegans* are protected from tumorous cell proliferation[6] and have reduced toxic protein aggregation[7], while *Drosophila* show less deterioration in their hearts[8]. Long-lived mouse mutants are protected from osteoporosis, cataracts and skin pathology, as well as decline in glucose homeostasis, immune and motor function[9]. The effect of these mutations is conserved from yeast to mammals, and it is, therefore, expected that if drugs replicate the biological impact of these changes, this could improve health in the elderly and prevent age-related disease. It is increasingly recognised that directly targeting ageing through pharmacological interventions, as opposed to specific age-related diseases, is a highly promising strategy for broad-spectrum disease protection[10]. However, at present, there are only a handful of reliable anti-ageing drugs whose effects have been confirmed in mammals, such as rapamycin[11] and metformin[12]. Crucially, there are currently no sufficiently reliable ageing biomarkers for testing drugs on human cells *in vitro,* and the development of a specialised epigenetic clock seems the most promising current approach[13,14,15].

To accelerate the discovery workflow for anti-ageing drugs, we took advantage of the breakthrough in the ageing field which showed that epigenetic clocks provide the most accurate measurements of human age, for instance, the approximate error rate for the Skin and Blood clock is ±2.5 years (maximal correlation coefficient 0,98)[13]. Epigenetic clocks surpass the accuracy of other ageing biomarkers such as telomere length and those based on transcriptomic, metabolomics or proteomic approaches, potentially because the latter approaches detect more transient and less stable cellular changes[16]. Ageing is accompanied by overall CpG hypomethylation, whilst some CpG islands and gene regions become hypermethylated[17]. Remarkably, only a small selection of the 56 million CpG sites in the diploid human genome, coupled with computational algorithms, is sufficient to provide an accurate readout of human age. One of the first epigenetic clocks was developed by Hannum using just 71 CpG sites to estimate age from blood samples[18], while Horvath's multi-tissue age estimator[16] and Skin and Blood clock[13] use 353 and 391 CpG sites, respectively[19,20]. Even a single CpG site in the ELOVL2 gene is sufficient to determine age[21], albeit clocks using only a few CpG sites are less accurate and less applicable to different tissues[19]. The epigenetic clocks measure the ageing

process inherent to all our cells and tissues, irrespective of their proliferation rate[14]. As the human epigenome reflects physiological changes, epigenetic clocks cannot only predict chronological age from a human sample but also give an estimate of biological age as has widely been demonstrated by the associations of epigenetic age with morbidity and mortality[19,22]. Recently, valuable predictors focussing on this aspect have been developed: PhenoAge[23] and GrimAge[24], which form the best epigenetic morbidity and mortality predictors available to date.

DNA methylation also captures information on the approximate number of cell divisions a stem cell has been through, as has been shown by epiTOC[25], a mitotic clock that approximates stem cell divisions and correlates with cancer risk[26]. The biology underlying CpG methylation alterations at the sites linked to ageing clocks is not well understood. Horvath suggests that it is linked to epigenetic maintenance programmes being reflected in DNA methylation alterations[16,19]. Some recent findings implicate loss of H3K36 histone methyltransferase NSD1 in epigenetic ageing clock acceleration [27]. Despite the enigma regarding epigenetic clock mechanism, these clocks are extremely useful and reliable predictors of age. However, little is known so far about the performance of these clocks in *in vitro* ageing experiments. It has recently been shown that the rate of epigenetic ageing in cultured cells is significantly faster than in the human body[14,28] and that epigenetic age is retarded by rapamycin *in vitro*[14], but neither of the clocks specialised for *in vitro* drug discovery nor were they tested on multiple anti-ageing drugs.

Therefore, we aimed to exploit the exceptional accuracy of CpG methylation clocks to uncover new anti-ageing pharmacological treatments. The current gold standard for discovering novel anti-ageing drugs are longevity experiments, which are laborious, lengthy and expensive. For instance, in mice, they take three years, thereby precluding any large scale drug screens. Existing screens in *C. elegans* commonly use live *E. coli* as food[29,30], which is a disadvantage as drugs are metabolised first by the bacteria making their effect on worms secondary, which may lead to confounded results[31,32]. Yeast drug screens lack the crucial aspect of tissue toxicity[33]. In addition, all longevity assays require constant supply of the drug, making them highly expensive. Other attempts to uncover anti-ageing effects of drugs are based on computational analysis using existing transcriptomic information on the ageing process combined with drug characteristics[34]. However, transcriptomic changes are more transient and noisy when compared to DNA methylation and are, therefore, a less consistent ageing marker[19].

We tested if existing epigenetic clocks could be used to measure anti-ageing drug potential in human primary cells *in vitro* and if we could build a new clock specialised for this purpose. Senescence is tightly associated with ageing of the organism, and because of the pronounced resemblance of ageing in primary cells *in vitro* to ageing *in vivo,* together with the evidence that human DNA methylation signatures are conserved and accelerated in cultured fibroblasts[28], we used cultured human cells as a proxy for human ageing[14,35]. The ability to test anti-ageing drug properties directly on human cells *in vitro* could considerably accelerate the discovery of new compounds promoting

121 healthy ageing. To this end, we used normal human mammary fibroblasts (HMFs) from a healthy 21-
122 year old donor that we cultured from passage 10 to passage 20, which is before these cells reach
123 senescence at passage 29 (Supplementary Fig. 1a-d). To measure CpG methylation, we used EPIC
124 Arrays (Illumina) that measure methylation at 850,000 sites.

125 First, we tested the three most suitable existing epigenetic clocks, to determine if they could detect
126 weekly and monthly ageing differences occurring during serial passaging of HMFs (Fig. 1a). The
127 Multi-tissue clock[16] consistently predicted a higher epigenetic age, and at passage ten this was
128 43.6±1.0 years (Fig. 1a), consistent with what was recently reported[28]. This increased age estimate,
129 compared to 16 years of the donor, is in accordance with published data demonstrating that this
130 epigenetic clock overestimates the age of mammary tissue samples[16]. The PhenoAge clock[23],
131 developed to predict mortality and morbidity risks, reported the epigenetic age of the donor to be
132 3.5±1.1 years younger (Fig. 1a). The most accurate age estimate, predicting the age of the donor at
133 23.2±0.87 years, was obtained using the Skin and Blood clock, which is specialised for determining
134 donor age of the cells in culture and of easily accessible human tissues (Fig. 1a). The Multi-tissue
135 clock and Skin and Blood clock showed a small increase in age with progressive passaging (from
136 passage 10 to 20, age estimate increased from 43.6±1.0 to 53.9±1.7 and from 23.2±0.87 to 31.6±1.2
137 years, respectively), whilst this increase was greater for the PhenoAge clock (from 3.5±1.1 to
138 26.6±9.7 years). This suggests that, of the tested clocks, the PhenoAge clock is most suitable to
139 measure ageing *in vitro* (Fig. 1a). However, the PhenoAge clock showed substantial variability in
140 predictions for higher passages, which would obstruct the detection of subtle ageing differences
141 upon anti-ageing drug treatments. In conclusion, while the Skin and Blood clock[13] measures
142 fibroblast ageing in culture, none of the existing clocks was ideally suited to accurately measure
143 subtle anti-ageing drug potential in human primary cells *in vitro,* and similar comparisons have
144 recently been reported by others[14,28].

145 This prompted us to develop a new clock that, rather than predicting donor age in years, specialises
146 in measuring methylation changes occurring during ageing of primary cells in culture and could
147 differentiate DNA methylation state between each passage. To this end, we developed a clock using
148 two different cell types, the above-mentioned HMFs and human dermal fibroblasts (HDFs), which
149 were obtained from a different donor, have a different proliferative lifespan *in vitro*, and a different
150 rate of DNA methylation change. Like the HMFs, the HDFs were serially passaged and sampled
151 every other passage for DNA methylation analysis (Fig. 1b). We filtered for significant probes using a
152 p-value threshold of $1x10^{-11}$, which gave the lowest error under our experimental setup, leaving
153 2,543 probes to build the clock using lasso regression, similar to the method used by Horvath[16]. We
154 then tested our novel epigenetic clock, which we named the CellAge clock, using an entirely different
155 set of samples, and we observed accurate prediction of passage number for both HMFs and HDFs,
156 with a Root Mean Square Error (RMSE) of 0.37 (Fig. 1c and Supplementary Fig. 2a).

157 Having built a precise epigenetic clock that measures methylation changes during replicative ageing
158 of human primary cells *in vitro*, we tested if anti-ageing drug treatment of HMFs and HDFs
159 decelerated the CellAge clock. We chose an mTOR inhibitor, rapamycin, which is one of the most
160 robust and evolutionarily conserved anti-ageing drug targets[36], and which mediates its effect through
161 down-regulation of S6K and Pol III, and up-regulation of autophagy[37,38]. We chose relatively low
162 rapamycin concentration of 5nM that did not inhibit cell growth (Supplementary Fig. 1a) but
163 moderately downregulated mTOR signalling, as evidenced by decreased pS6K and p4E-BP
164 phosphorylation (Supplementary Fig. 3). This setup mimics the pro-longevity effects of rapamycin *in*
165 *vivo* where it is well accepted that only mild nutrient sensing pathway inhibition increases life- and
166 healthspan[5,39]. DNA methylation profiles from HMFs collected following four, six and eight weeks of
167 rapamycin treatment (passage 16, 18 and 20; Fig. 2) were analysed using the CellAge clock and
168 clearly demonstrated that rapamycin slows down methylation changes associated with replicative
169 ageing. Interestingly, this clock deceleration was more pronounced upon longer treatment as shown
170 by the gradual decrease of predicted-actual passage from 16 to 20 weeks. The low dose rapamycin
171 treatment did not affect population doublings, confirming that the methylation changes were not a
172 reflection of proliferation inhibition or slowing of the cell cycle (Supplementary Fig. 1). This is further
173 evidenced by comparing the predicted passage from the CellAge clock against cumulative
174 population doubling, showing rapamycin samples lie on a separate line to that of the control samples
175 (Supplementary Fig. 2b,c). Contrarily, rapamycin samples and controls differed to considerably
176 lesser extent when actual passage and cumulative population doublings are compared
177 (Supplementary Fig. 2b,c). Importantly, we observed a similar pattern for HMFs and HDFs (Fig. 2),
178 suggesting that the CellAge clock could be applicable to different cells, albeit calibration is required
179 for cells that reach senescence at different rates.

180 We then focused on HMFs to test another anti-ageing drug, trametinib[40], an inhibitor of the
181 MEK/ERK signalling pathway, which we also applied in low concentration to avoid any effect on
182 growth and population doubling (Supplementary Fig. 1 and Fig. 3). The CellAge clock analysis of
183 trametinib treatment showed clock deceleration for all three passages tested (Fig. 2), thereby
184 confirming previous results in *Drosophila in vivo* that trametinib extends lifespan[40]. Next, we
185 examined the effect of two other inhibitors of nutrient-sensing pathways as mutations in these
186 pathways in model organisms represent the most evolutionary conserved anti-ageing interventions[5].

187 We tested Dactolisib/BEZ235, a dual ATP competitive PI3K and mTOR inhibitor, for which we again
188 optimised the dose of the treatment to obtain a reduction in signalling without significant proliferation
189 impairment, as shown by pS6K downstream target 4E-BP (Supplementary Fig. 3).
190 Dactolisib/BEZ235 slowed down the DNA methylation changes similar to rapamycin, suggesting that
191 Dactolisib/BEZ235 could be a new anti-ageing drug according to the output of the CellAge clock (Fig.
192 2). We also tested torin2, which is a selective inhibitor of the mTOR pathway that inhibits both
193 mTORC1 and mTORC2, unlike rapamycin, which targets solely mTORC1. Owing to its more

complete inhibition of the mTOR pathway, we were interested in examining its effect on replicative ageing, especially as the role of mTORC2 in ageing is less well established. The impact of mTORC2 inhibition on lifespan can be positive or negative depending on which of the mTORC2 downstream effectors is affected, in which tissue, and whether females or male mice are used for the experiment[41]. Some of the negative effects of mTOR pathway inhibition, such as insulin resistance and hyperlipidemia, are attributed to the mTORC2 branch of the pathway and may arise under certain conditions of prolonged and/or high dose rapamycin treatment[41]. Interestingly, while our CellAge clock suggests that torin2 is indeed a novel anti-ageing drug (Fig. 2), its effect on ageing in mammalian cell culture appears to be less pronounced than that of rapamycin. This is in line with literature suggesting that a promising strategy to improve healthy ageing is the development of inhibitors that are highly specific for mTORC1 or that target mTORC1 downstream effectors separately[41].

Next, we compared our anti-ageing drug screening results obtained by the CellAge clock with analyses using Horvath's Multi-tissue and Skin and Blood clock, as well as the PhenoAge clock. The clocks did not detect any significant effect of anti-ageing drug treatment (Supplementary Fig. 4). The Skin and Blood clock[26] was used recently to measure deceleration of ageing in primary fibroblasts[14,28], however the concentration of rapamycin used in our conditions was five times lower without effect on cell growth, highlighting the sensitivity of our epigenetic clock to detect age-related methylation changes at very low drug concentrations. Under our conditions, the only epigenetic clock that detected gradual methylation changes from passage 10 to passage 20 was the PhenoAge clock (Supplementary Fig. 4). However, its output was more variable between samples and inconsistent for anti-ageing drug treatments, reporting both clock acceleration and deceleration. For instance, rapamycin, Dactolisib/BEZ235 and torin2 treated cells appeared slightly younger compared to controls, whereas trametinib treated cells were estimated older to some extent (Supplementary Fig. 4), unlike the results we obtained with our CellAge clock (Fig. 2). Overall, the CellAge clock that we developed here was more consistent and performed significantly better on ageing cells in culture and following known anti-ageing drug treatments compared to existing clocks, as evidenced by its ability to detect subtle ageing differences. Our results are supportive of clocks being highly specialised for a certain task, and suggests that while other popular epigenetic clocks perform remarkably on determining donor's age in years and their health status, they were not able to robustly detect slight ageing changes in human primary cells induced by drug treatment over a short period of time *in vitro*.

Next, we assessed if the CellAge clock is suitable for the screening of novel anti-ageing drugs. To this aim, we examined if drugs that decelerate the CellAge clock also reduce features associated with senescence, such as morphological changes and expression of ageing biomarkers[42]. Rapamycin, Dactolisib/BEZ235 and Trametinib treatment slowed down morphological alteration in cells that gradually occur during replicative ageing, namely cell elongation, increased nuclear area

231 and cell area, and the treated cells appeared particularly 'youthful' (Fig. 3). Another characteristic of
232 senescence is increased expression of the cyclin-dependent kinase inhibitors $p21^{CIP1/Waf1}$ and
233 $p16^{INK4a}$. $p21^{CIP1/Waf1}$ triggers G1 cycle arrest upon damage and can lead to senescence or
234 apoptosis[43,44]. Expression of $p16^{INK4a}$, which is produced from the CDKN2A gene together with
235 $p19^{ARF}$ ($p14^{ARF}$ in humans) increases exponentially during ageing and was suggested to stabilise the
236 senescent state[45]. $p16^{INK4a}$ expression was the marker of choice for senescent cell clearance leading
237 to prolonged lifespan in mice[46]. Our results demonstrate that drugs which decelerate the CellAge
238 clock at the same time reduce expression of both nuclear $p21^{CIP1/Waf1}$ and $p16^{INK4a}$ compared to non-
239 treated cells, showing their efficacy in delaying the senescence programme (Fig. 3b,c). In addition,
240 the most frequently used senescent marker, senescent-associated β-galactosidase activity (SA-
241 βgal), was significantly decreased upon anti-ageing drugs treatment with rapamycin and
242 Dactolisib/BEZ235, but not in cells treated with trametinib (Fig. 3b,c). Another difference in
243 senescent markers was observed with interleukin-6 (IL-6), which is one of the most important
244 inflammatory cytokines and part of the senescent-associated secretory phenotype. IL-6 was
245 significantly reduced in aged cells upon rapamycin and Dactolisib/BEZ235 treatment but not in
246 trametinib treated cells (Fig. 3b,c). This difference possibly stems from the overactivated RAS/ERK
247 pathway being a more prominent inducer of senescence than the overactivated mTOR/PI3K
248 pathway[47], and hence corresponding inhibitors have different potency in inhibiting senescence.
249 Finally, we examined the nucleolus, an organelle dedicated to rRNA production and ribosomal
250 assembly, as it has recently emerged that maintenance of its structure, and low levels of nucleolar
251 methyltransferase fibrillarin, is a common denominator for major anti-ageing intervention from worms
252 to mice[48]. We observed that as a consequence of ageing, nucleoli in aged HMFs lose their defined
253 round shape, are more diffused, and stain less well. For rapamycin and Dactolisib/BEZ235, we
254 observed clearly defined and 'younger' looking nucleoli in aged cells. However, trametinib treated
255 cells resembled the nucleoli of controls. In summary, a panel of the most frequently used markers for
256 cell senescence confirmed that drugs which decelerate the CellAge clock also make the cells appear
257 more youthful. This strongly suggests that the CellAge clock can be used as a robust and sensitive
258 detector of novel anti-ageing treatments.

259 Finally, having discovered two novel potential anti-ageing drug treatments using the CellAge clock,
260 Dactolisib/BEZ235 and torin2, we tested and validated them *in vivo* using the fruit fly *Drosophila*
261 *melanogaster* as a model organism. This is important as tissue-specific drug toxicity, which can be
262 missed in cell culture, is one of the major reasons for drug failure in clinical trials. For *in vivo*
263 longevity studies we used the outbred wild-type w^{Dah} strain which is particularly suitable for ageing
264 studies, Drosoflipper device for fast fly transfer, and specially formulated holidic medium[49] to
265 increase drug bioavailability compared to standard sugar-yeast-agar fly food. We used rapamycin as
266 a positive control for longevity experiments in flies and showed that median lifespan extension on
267 holidic media varied from 7% to 9% compared to ethanol solvent control, depending on 1μM or 5μM
268 concentration, respectively ($p<0.001$, log-rank test), which is comparable to published literature[50]

269 (Fig. 4a). Importantly, both Dactolisib/BEZ235 and torin2 significantly extended lifespan in
270 *Drosophila* for 7% ($p<0.001$, log-rank test) (Fig. 4b,c). This firmly demonstrates that drugs that
271 decelerate the CellAge clock have similarly favourable output on major anti-ageing biomarkers *in*
272 *vitro* and extend longevity *in vivo*.

273 For the first time, we have a robust epigenetic clock for the rapid discovery of anti-ageing drugs
274 directly in human cells, bypassing lower model organisms and significantly shortening discovery time
275 compared to 3-year long mice longevity analysis. Testing different compounds for ageing using the
276 CellAge clock could potentially reveal new anti-ageing pathways and help us to improve our
277 knowledge base of not only ageing biology but of molecular pathways underpinning the epigenetic
278 clocks as well, understanding of which is limited. Other available epigenetic clocks could not detect
279 anti-ageing drugs so accurately. The CellAge clock, however, does not predict the chronological age
280 of the sample, demonstrating that epigenetic clocks are highly specialised to the purpose for which
281 they were trained. We expect many biological outputs to be extracted by different epigenetic clock
282 algorithms in the future, given the wealth of information stored in our epigenome.
283
284 Better experimental systems to test anti-ageing drugs are very much needed, given a rising
285 proportion of the elderly in modern societies and, as a consequence, larger numbers of people
286 suffering from age-related diseases. Our results show that by using the CellAge clock, cultured
287 primary human cells can be used as a proxy to measure human ageing and can reliably detect anti-
288 ageing effects upon a relatively brief treatment. By doing so, this fast and accurate method is
289 expected to accelerate the discovery of novel preventive treatments for age-related disease, directly
290 using human cells. Importantly, further research will be focused on expanding our findings on
291 different types of primary cells from donors with different ages, as well as on testing various
292 compounds. While ageing itself is not a disease, potential anti-ageing drugs could be FDA approved
293 separately for different conditions. The first study to test broad-spectrum protection capacity of
294 metformin, the TAME study, is underway[51]. In addition, it was shown that rapamycin/everolimus pre-
295 treatment dramatically improves flu vaccination and immune response in the elderly[52]. In mice, it
296 also lowers the incidence of tumours[53], and it shows promising results in the field of
297 neurodegeneration[54]. This supports the idea that targeting healthy ageing might have multiple
298 beneficial outputs.
299
300 Our novel drug discovery platform will inform on new anti-ageing mechanisms, currently dominated
301 by IIS and mTOR signalling pathways as well as dietary restriction regimes, and will thereby
302 advance our understanding of the ageing process. Many drugs targeting growth pathways are
303 already available from cancer research where they are used in very high doses. With our CellAge
304 clock, it could be examined which of these compounds can be disease preventative at very low
305 concentrations. Our experimental setup is also suitable for nutraceutical approaches whereby dietary
306 supplements could be rigorously tested for their effect on ageing. Overall, we expect our accelerated

307 discovery platform to be valuable for the discovery of strongly sought after anti-ageing drugs and
308 geroprotective strategies to improve healthy human ageing.
309

310 Methods

311 **Cell culture and reagents.** Normal finite lifespan human mammary fibroblasts (HMFs) were
312 obtained from reduction mammoplasty tissue of a 16-year-old individual, donor 48 by Dr Martha
313 Stampfer (University Berkeley) who has all required IRB approvals to distribute these cell
314 samples and MTA agreement set in place with Dr Cleo Bishop laboratory. Independent cultures
315 from these cells were serially passaged from passage 9 through to passage 20 and aliquots
316 taken upon each passage for Illumina Infinium Methylation EPIC analysis. HMFs were
317 maintained in Dulbecco's Modified Eagles Medium (DMEM) (Life Technologies, UK)
318 supplemented with 10% foetal bovine serum (FBS) (Labtech.com, UK), 2mM L-glutamine (Life
319 Technologies, UK) and 10 µg/mL insulin from bovine pancreas (Sigma).
320 Normal finite lifespan human dermal fibroblasts (HDFs) were obtained from face lift dermis
321 following a kind donation from an anonymous healthy patient under standard ethical practice,
322 reference LREC No. 09/HO704/69. HDFs were grown in DMEM with 4 mM L-glutamine (Life
323 Technologies), supplemented with 10% FBS.
324 Cells were plated at 7,500 cells/cm^2 in T25 cell culture flask in 5ml of media to which 5µl of
325 appropriate drug or vehicle control was added. Media was changed every two days and cells
326 were passaged every 7 days and trypsinisation was used to detach the cells. All cells were
327 routinely tested for mycoplasma and shown to be negative.
328
329
330 **Immunofluorescence microscopy and high content analysis.** Cells were washed in
331 phosphate buffered saline (PBS), fixed for 15 minutes with 3.7% paraformaldehyde with 5%
332 sucrose, washed and permeabilised for 15 minutes using 0.1% Triton X in PBS (30 minutes
333 for anti-nucleolin antibody) then washed and blocked in 0.25% bovine serum albumin (BSA)
334 in PBS before primary antibody incubations. Primary antibodies used were anti-IL6 (R&D
335 Systems, 1:100; overnight 4°C), anti-nucleolin (Santa Cruz, 1:2000, overnight room
336 temperature), anti-p16 (Proteintech, 1:500, overnight 4°C), anti-p21 (12D1, Cell Signalling,
337 1:2000, overnight 4°C). Cells were incubated for 2 hours at room temperature with the
338 appropriate AlexaFluor-488, AlexaFluor-546 or AlexaFluor-647 conjugated antibody (1:500,
339 Invitrogen), DAPI (1:1,000 from 1mg/mL stock) and CellMask Orange or Deep Red
340 (1:200,000, Invitrogen). Images were acquired using the IN Cell 2200 or 6000 automated
341 microscope (GE) and HCA was performed using the IN Cell Developer software (GE).
342

343 **Z score generation.** For each of the parameters analysed, significance was defined as
344 one Z score from the negative control mean. Z scores were generated according to the
345 formula below: Z score = (mean value of experimental condition – mean value of vehicle
346 control/standard deviation (SD) for vehicle control.
347
348 **Senescence-associated beta-galactosidase (SA-β-Gal) assay.** Cells were washed in
349 PBS, fixed for 5 minutes with 0.2% glutaraldehyde, washed and incubated for 24 hour at
350 37°C (no CO_2) with fresh senescence-associated beta-galactosidase (SA-β-Gal) solution:
351 1mg of 5-bromo-4-chloro-3-indoyl β-D-galactosidase (X-Gal) per mL (stock = 20mg of
352 dimethylsulfoxide per ml) / 40mM citric acid/sodium phosphate, pH 6.0 / 5mM potassium
353 ferrocyanide / 5mM potassium ferricyanide / 150mM NaCl / 2mM $MgCl_2$). Cells were
354 stained with Hoechst 33342 (1:10,000 from 10mg/mL stock) for 30 minutes. Images were
355 acquired using the IN Cell 2200 automated microscope and HCA was performed using the
356 IN Cell Developer software.
357
358 **Genomic DNA extraction.** For isolation of Genomic DNA from primary human fibroblasts
359 we used QIAamp DNA micro kit (56304) and we followed manufacturers protocol, with an
360 additional washing steps with 500μl AW2 buffer and 500μl 80% ethanol to improve purity.
361 DNA quantification and purity was determined by Nanodrop and QuBit. For bisulfite
362 conversion EZ DNA methylation kit was used (D5001).
363
364 **Preparation of methylation array data.** For each sample, 500ng high-quality DNA was
365 bisulphite converted using the EZ DNA methylation kit (Zymo Research), using the
366 alternative incubation conditions recommended for use with Illumina methylation arrays.
367 Bisulphite converted DNA was eluted in 12ul elution buffer. Methylation was analysed using
368 the Infinium Human Methylation EPIC array (Illumina) using standard operating procedures
369 at the UCL Genomics facility. The EPIC array data have been deposited into ArrayExpress
370 at the European Bioinformatics Institute (https://www.ebi.ac.uk/arrayexpress/) under
371 accession number E-MTAB-8327.
372 .
373
374 **Pre-processing of methylation array data.** DNA methylation array data was processed
375 using the minfi package[55] within R (http://www.R-project.org/). Initial QC metrics from this
376 package were used to remove low-quality samples. Probes were filtered using a detection
377 p-value cut-off >0.01 and normalised using the Noob procedure. Cross-hybridising probes

378 were removed from analysis based on the list published in McCartney et al.[56] The training
379 and test sets were pre-processed separately to obtain a fair estimate of the performance of
380 CellAge clock.
381
382 **Estimation of sample age using existing epigenetic clocks.** Following pre-processing
383 of data, the epigenetic age of all samples was predicted using three epigenetic clocks; the
384 Multi-tissue clock[16], the Skin and Blood clock[13] and the PhenoAge clock[23].
385
386 **Development of the CellAge clock.** The clock was built using a total of 39 samples, with
387 6 samples at each of the following passages; 10,12, and 14 and 7 samples at each of the
388 following passages; 16, 18, and 20. This included both dermal fibroblasts (n=12) and
389 mammary fibroblasts (n=27). Probes were initially filtered from the 730,453 available using
390 the dmpFinder function within minfi[55]. A p-value threshold was used to determine which
391 probes to use in the model building and this was selected using a leave one out validation,
392 yielding the threshold of $1x10^{-11}$ and a total of 2,543 probes. We built the model using
393 elastic net regression (setting alpha=0.5) from the glmnet package[57] within R and
394 determining the lambda parameter using internal cross validation function provided.
395
396 **Lifespan measurements.** We used *white Dahomey* (w^{Dah}) wild-type flies that were
397 maintained and all experiments were conducted at 25ºC. Flies were kept on a 12 h light:12
398 h dark cycle at constant humidity using standard sugar/yeast/agar (SYA) medium. For all
399 experiments, flies were reared at standard larval density by transferring 18 *µ*l of egg
400 suspension into SYA bottles. Eclosing adults were collected over a 12-h period and allowed
401 to mate for 48 h before sorting into single sexes and placed in vials containing either control
402 or experimental drug food. For lifespan assays, flies were reared at standard density and
403 maintained at 15 flies per vial and we used holidic media recipe food for all longevity
404 assays[49]. Flies were transferred to fresh food vials every 2-3 days and scored for deaths. At
405 least 150 flies were used for each lifespan experiment.
406
407 **Western blot measurements.** Whole flies or human primary cell pellet was homogenised
408 in 2x Laemmli loading sample buffer (100 mM Tris pH 6.8, 20% glycerol, 4% SDS; Bio-Rad)
409 containing 50 mM DTT. Extracts were cleared by centrifugation and approximately 20 µg of
410 protein extract was loaded per lane on a polyacrylamide gel. Proteins were separated and
411 transferred to nitrocellulose membrane. The following antibodies were used at the indicated
412 dilutions: H3 (Cell Signaling Technology; 1:2000; 4499S), pS6K (Cell Signaling Technology;

413 1:1000; 9206S), total S6K (Santa Cruz; 1:1000; 8418), p4EBP (Cell Signalling Technology,
414 1:500; 2855S), non-phospho4E-BP (Cell Signalling Technology; 1:500; 4923S), pAkt (Cell
415 Signalling; 1:1000; 4060), pAkt (Cell Signalling; 1:1000; 4056), total Akt (Cell Signalling;
416 1:1000; 9272), pERK (Cell Signalling; 1:1000; 4370), total (Cell Signalling; 1:1000; 4692).
417 Blots were developed using the ECL detection system (GE, Amersham), and analysed
418 using FIJI software (US National Institutes of Health). We used precasted TGX stain-free
419 gels from Bio-Rad (567-8123 or 567-8124) according to the manufacturer's instructions.
420
421 **Statistical analysis.** Statistical analysis was performed using JMP software (version 4.0.5;
422 SAS Institute) and R. Log-rank tests were performed on lifespan curves. Probes were
423 selected to build CellAge using an F-test and CellAge was built using lasso regression.

424 **Online content**

425 The code for CellAge clock is available from GitHub. All methylation microarray data reported
426 in this study have been deposited in the ArrayExpress
427 (https://www.ebi.ac.uk/arrayexpress/) public repository and they are accessible under
428 accession number E-MTAB-8327.
429

430 **References**

431

432 1 Wilson, B. E. *et al.* Estimates of global chemotherapy demands and corresponding
433 physician workforce requirements for 2018 and 2040: a population-based study.
434 *Lancet Oncol* **20**, 769-780, doi:10.1016/S1470-2045(19)30163-9 (2019).
435 2 Reeve, A., Simcox, E. & Turnbull, D. Ageing and Parkinson's disease: why is
436 advancing age the biggest risk factor? *Ageing Res Rev* **14**, 19-30,
437 doi:10.1016/j.arr.2014.01.004 (2014).
438 3 Partridge, L., Deelen, J. & Slagboom, P. E. Facing up to the global challenges of
439 ageing. *Nature* **561**, 45-56, doi:10.1038/s41586-018-0457-8 (2018).
440 4 Rae, M. J. *et al.* The demographic and biomedical case for late-life interventions in
441 aging. *Sci Transl Med* **2**, 40cm21, doi:2/40/40cm21 [pii]
442 10.1126/scitranslmed.3000822 (2010).
443 5 Lopez-Otin, C., Blasco, M. A., Partridge, L., Serrano, M. & Kroemer, G. The
444 hallmarks of aging. *Cell* **153**, 1194-1217, doi:S0092-8674(13)00645-4 [pii]
445 10.1016/j.cell.2013.05.039 (2013).

446 6 Pinkston, J. M., Garigan, D., Hansen, M. & Kenyon, C. Mutations that increase the
447 life span of C. elegans inhibit tumor growth. *Science* **313**, 971-975 (2006).
448 7 Cohen, E., Bieschke, J., Perciavalle, R. M., Kelly, J. W. & Dillin, A. Opposing
449 activities protect against age-onset proteotoxicity. *Science* **313**, 1604-1610 (2006).
450 8 Wessells, R. J., Fitzgerald, E., Cypser, J. R., Tatar, M. & Bodmer, R. Insulin
451 regulation of heart function in aging fruit flies. *Nat Genet* **36**, 1275-1281 (2004).
452 9 Selman, C. *et al.* Evidence for lifespan extension and delayed age-related
453 biomarkers in insulin receptor substrate 1 null mice. *Faseb J* **22**, 807-818 (2008).
454 10 Niccoli, T. & Partridge, L. Ageing as a risk factor for disease. *Curr Biol* **22**, R741-
455 752, doi:S0960-9822(12)00815-9 [pii]
456 10.1016/j.cub.2012.07.024 (2012).
457 11 Harrison, D. E. *et al.* Rapamycin fed late in life extends lifespan in genetically
458 heterogeneous mice. *Nature* **460**, 392-395, doi:nature08221 [pii]
459 10.1038/nature08221 (2009).
460 12 Martin-Montalvo, A. *et al.* Metformin improves healthspan and lifespan in mice. *Nat*
461 *Commun* **4**, 2192, doi:10.1038/ncomms3192 (2013).
462 13 Horvath, S. *et al.* Epigenetic clock for skin and blood cells applied to Hutchinson
463 Gilford Progeria Syndrome and ex vivo studies. *Aging (Albany NY)* **10**, 1758-1775,
464 doi:10.18632/aging.101508 (2018).
465 14 Horvath, S., Lu, A. T., Cohen, H. & Raj, K. Rapamycin retards epigenetic ageing of
466 keratinocytes independently of its effects on replicative senescence, proliferation
467 and differentiation. *Aging (Albany NY)* **11**, 3238-3249, doi:10.18632/aging.101976
468 (2019).
469 15 Castillo-Quan, J. I., Kinghorn, K. J. & Bjedov, I. Genetics and pharmacology of
470 longevity: the road to therapeutics for healthy aging. *Adv Genet* **90**, 1-101,
471 doi:S0065-2660(15)00005-X [pii]
472 10.1016/bs.adgen.2015.06.002 (2015).
473 16 Horvath, S. DNA methylation age of human tissues and cell types. *Genome Biol* **14**,
474 R115, doi:gb-2013-14-10-r115 [pii]
475 10.1186/gb-2013-14-10-r115 (2013).
476 17 Booth, L. N. & Brunet, A. The Aging Epigenome. *Mol Cell* **62**, 728-744,
477 doi:10.1016/j.molcel.2016.05.013 (2016).
478 18 Hannum, G. *et al.* Genome-wide methylation profiles reveal quantitative views of
479 human aging rates. *Mol Cell* **49**, 359-367, doi:S1097-2765(12)00893-3 [pii]
480 10.1016/j.molcel.2012.10.016 (2013).

481 19 Horvath, S. & Raj, K. DNA methylation-based biomarkers and the epigenetic clock
482 theory of ageing. *Nat Rev Genet* **19**, 371-384, doi:10.1038/s41576-018-0004-3
483 (2018).
484 20 Field, A. E. *et al.* DNA Methylation Clocks in Aging: Categories, Causes, and
485 Consequences. *Mol Cell* **71**, 882-895, doi:10.1016/j.molcel.2018.08.008 (2018).
486 21 Garagnani, P. *et al.* Methylation of ELOVL2 gene as a new epigenetic marker of
487 age. *Aging Cell* **11**, 1132-1134, doi:10.1111/acel.12005 (2012).
488 22 Marioni, R. E. *et al.* DNA methylation age of blood predicts all-cause mortality in
489 later life. *Genome Biol* **16**, 25, doi:10.1186/s13059-015-0584-6 (2015).
490 23 Levine, M. E. *et al.* An epigenetic biomarker of aging for lifespan and healthspan.
491 *Aging (Albany NY)* **10**, 573-591, doi:10.18632/aging.101414 (2018).
492 24 Lu, A. T. *et al.* DNA methylation GrimAge strongly predicts lifespan and healthspan.
493 *Aging (Albany NY)* **11**, 303-327, doi:10.18632/aging.101684 (2019).
494 25 Yang, Z. *et al.* Correlation of an epigenetic mitotic clock with cancer risk. *Genome*
495 *Biol* **17**, 205, doi:10.1186/s13059-016-1064-3
496 10.1186/s13059-016-1064-3 [pii] (2016).
497 26 Tomasetti, C., Li, L. & Vogelstein, B. Stem cell divisions, somatic mutations, cancer
498 etiology, and cancer prevention. *Science* **355**, 1330-1334, doi:355/6331/1330 [pii]
499 10.1126/science.aaf9011 (2017).
500 27 Martin-Herranz, D. E. *et al.* Screening for genes that accelerate the epigenetic aging
501 clock in humans reveals a role for the H3K36 methyltransferase NSD1. *Genome*
502 *Biol* **20**, 146, doi:10.1186/s13059-019-1753-9 (2019).
503 28 Sturm, G. *et al.* Human aging DNA methylation signatures are conserved but
504 accelerated in cultured fibroblasts. *Epigenetics*, 1-16,
505 doi:10.1080/15592294.2019.1626651 (2019).
506 29 Ye, X., Linton, J. M., Schork, N. J., Buck, L. B. & Petrascheck, M. A
507 pharmacological network for lifespan extension in Caenorhabditis elegans. *Aging*
508 *Cell* **13**, 206-215, doi:10.1111/acel.12163 (2014).
509 30 Lucanic, M., Lithgow, G. J. & Alavez, S. Pharmacological lifespan extension of
510 invertebrates. *Ageing Res Rev* **12**, 445-458, doi:10.1016/j.arr.2012.06.006 (2013).
511 31 Cabreiro, F. *et al.* Metformin retards aging in C. elegans by altering microbial folate
512 and methionine metabolism. *Cell* **153**, 228-239, doi:10.1016/j.cell.2013.02.035
513 (2013).

514 32 Pryor, R. *et al.* Host-Microbe-Drug-Nutrient Screen Identifies Bacterial Effectors of
515 Metformin Therapy. *Cell* **178**, 1299-1312 e1229, doi:10.1016/j.cell.2019.08.003
516 (2019).
517 33 Zimmermann, A. *et al.* Yeast as a tool to identify anti-aging compounds. *FEMS*
518 *Yeast Res* **18**, doi:10.1093/femsyr/foy020 (2018).
519 34 Donertas, H. M., Fuentealba Valenzuela, M., Partridge, L. & Thornton, J. M. Gene
520 expression-based drug repurposing to target aging. *Aging Cell* **17**, e12819,
521 doi:10.1111/acel.12819 (2018).
522 35 Lowe, R. *et al.* The senescent methylome and its relationship with cancer, ageing
523 and germline genetic variation in humans. *Genome Biol* **16**, 194,
524 doi:10.1186/s13059-015-0748-4 (2015).
525 36 Saxton, R. A. & Sabatini, D. M. mTOR Signaling in Growth, Metabolism, and
526 Disease. *Cell* **168**, 960-976, doi:10.1016/j.cell.2017.02.004 (2017).
527 37 Bjedov, I. *et al.* Mechanisms of life span extension by rapamycin in the fruit fly
528 Drosophila melanogaster. *Cell Metab* **11**, 35-46, doi:S1550-4131(09)00374-X [pii]
529 10.1016/j.cmet.2009.11.010 (2010).
530 38 Filer, D. *et al.* RNA polymerase III limits longevity downstream of TORC1. *Nature*
531 **552**, 263-267, doi:10.1038/nature25007 (2017).
532 39 Bjedov, I. & Partridge, L. A longer and healthier life with TOR down-regulation:
533 genetics and drugs. *Biochem Soc Trans* **39**, 460-465, doi:BST0390460 [pii]
534 10.1042/BST0390460 (2011).
535 40 Slack, C. *et al.* The Ras-Erk-ETS-Signaling Pathway Is a Drug Target for Longevity.
536 *Cell* **162**, 72-83, doi:S0092-8674(15)00707-2 [pii]
537 10.1016/j.cell.2015.06.023 (2015).
538 41 Kennedy, B. K. & Lamming, D. W. The Mechanistic Target of Rapamycin: The
539 Grand ConducTOR of Metabolism and Aging. *Cell Metab* **23**, 990-1003,
540 doi:10.1016/j.cmet.2016.05.009 (2016).
541 42 Hanzelmann, S. *et al.* Replicative senescence is associated with nuclear
542 reorganization and with DNA methylation at specific transcription factor binding
543 sites. *Clin Epigenetics* **7**, 19, doi:10.1186/s13148-015-0057-5 (2015).
544 43 He, S. & Sharpless, N. E. Senescence in Health and Disease. *Cell* **169**, 1000-1011,
545 doi:10.1016/j.cell.2017.05.015 (2017).
546 44 McHugh, D. & Gil, J. Senescence and aging: Causes, consequences, and
547 therapeutic avenues. *J Cell Biol* **217**, 65-77, doi:10.1083/jcb.201708092 (2018).

45 Gire, V. & Dulic, V. Senescence from G2 arrest, revisited. *Cell Cycle* **14**, 297-304, doi:10.1080/15384101.2014.1000134 (2015).

46 Baker, D. J. *et al.* Naturally occurring p16(Ink4a)-positive cells shorten healthy lifespan. *Nature* **530**, 184-189, doi:10.1038/nature16932 (2016).

47 Kennedy, A. L. *et al.* Activation of the PIK3CA/AKT pathway suppresses senescence induced by an activated RAS oncogene to promote tumorigenesis. *Mol Cell* **42**, 36-49, doi:10.1016/j.molcel.2011.02.020 (2011).

48 Tiku, V. & Antebi, A. Nucleolar Function in Lifespan Regulation. *Trends Cell Biol* **28**, 662-672, doi:10.1016/j.tcb.2018.03.007 (2018).

49 Piper, M. D. *et al.* A holidic medium for Drosophila melanogaster. *Nat Methods* **11**, 100-105, doi:10.1038/nmeth.2731 (2014).

50 Fan, X. *et al.* Rapamycin preserves gut homeostasis during Drosophila aging. *Oncotarget* **6**, 35274-35283, doi:10.18632/oncotarget.5895 (2015).

51 Barzilai, N., Crandall, J. P., Kritchevsky, S. B. & Espeland, M. A. Metformin as a Tool to Target Aging. *Cell Metab* **23**, 1060-1065, doi:S1550-4131(16)30229-7 [pii] 10.1016/j.cmet.2016.05.011 (2016).

52 Mannick, J. B. *et al.* TORC1 inhibition enhances immune function and reduces infections in the elderly. *Sci Transl Med* **10**, doi:10.1126/scitranslmed.aaq1564 (2018).

53 Anisimov, V. N. *et al.* Rapamycin increases lifespan and inhibits spontaneous tumorigenesis in inbred female mice. *Cell Cycle* **10**, 4230-4236, doi:18486 [pii] 10.4161/cc.10.24.18486 (2011).

54 Bove, J., Martinez-Vicente, M. & Vila, M. Fighting neurodegeneration with rapamycin: mechanistic insights. *Nat Rev Neurosci* **12**, 437-452, doi:10.1038/nrn3068 (2011).

55 Fortin, J. P., Triche, T. J., Jr. & Hansen, K. D. Preprocessing, normalization and integration of the Illumina HumanMethylationEPIC array with minfi. *Bioinformatics* **33**, 558-560, doi:10.1093/bioinformatics/btw691 (2017).

56 McCartney, D. L. *et al.* Identification of polymorphic and off-target probe binding sites on the Illumina Infinium MethylationEPIC BeadChip. *Genom Data* **9**, 22-24, doi:10.1016/j.gdata.2016.05.012 (2016).

57 Friedman, J., Hastie, T. & Tibshirani, R. Regularization Paths for Generalized Linear Models via Coordinate Descent. *J Stat Softw* **33**, 1-22 (2010).

Acknowledgements

IB acknowledges funding from ERC StG 311331, ERC PoC 842174, Royal Society Research Grant, The Bill Lyons foundation. This work was supported in part by the CRUK-UCL Centre Award [C416/A25145] awarded to IB and SB. EJT has been funded by MRC (MR/K501372/1) and BBSRC (BB/P002579/1) and DM is funded by the BBSRC (BB/N503629/1). JG, and MS are supported by U.S. Department of Energy under Contract No. DE-AC02-05CH11231 and the Congressionally Directed Medical Research Programs Breast Cancer Research Program Era of Hope Scholar Award BC141351.

Authors contribution

SB, IB developed initial concept. SB, IB, RL and CLB finalised concept developing and designed experiments. RL and APW analysed data. RL developed CellAge clock. CLB and EJT provided cell culture expertise. CL, EJT, ERS, VEMM, DM and IB performed all experiments. SE, SB, IB, RL, CLB wrote the manuscript. JCG and MRS provided critical reagents. All authors discussed results and commented on and approved the manuscript.

Competing interest

The authors declare no competing interest.

Additional information

Correspondence and requests for materials should be addressed to IB, CLB, RL and SB.

Figure Legends

Figure 1. Development of CellAge clock for monitoring subtle ageing difference in cells in culture.

A) Predicted age of control samples using three existing epigenetic clocks. Predicted epigenetic age for control samples across all experiments as estimated by the Multi-tissue clock (green), the Skin and Blood clock (orange) and the PhenoAge clock (yellow). All three clocks show a trend to increase in predicted age with progressing passage, however there is a lot of variability in predictions, particularly for the PhenoAge clock. The Multi-tissue clock consistently predicted cells to have the highest epigenetic age, while the PhenoAge clock consistently predicted cells to

612 have the lowest epigenetic age, which even reached below zero for several samples
613 at various passages.
614 B) Genome-wide methylation changes upon cell passages of primary human
615 mammary fibroblasts (HMF) and primary human dermal fibroblast (HDF).
616 C) Testing the CellAge clock on HMF and HDF samples that were not used to train the
617 clock, demonstrates accurate prediction of the cell passage.
618
619 **Figure 2.** Using the CellAge clock for the detection of anti-ageing drugs.
620 A) The methylome of Human Dermal Fibroblasts (HDF) and
621 B) Human Mammary Fibroblasts (HMF) was analysed using the CellAge clock.
622 Represented is Predicted-Actual Passage for Passage 16, 18 and 20, showing
623 deceleration of CellAge upon treatment with anti-ageing drugs rapamycin (5nM),
624 Dactolisib/BEZ235 (10nM), torin2 (5nM) and Trametinib (0.1nM).

625
626 **Figure 3.** Treatment with anti-ageing drugs decreases markers of senescence.
627 A) Schematic illustrating the experimental set-up conducted in P10 to P22 HMFs,
628 passaged weekly.
629 B) Multi-parameter analysis of senescence markers. Colour coding used to illustrate
630 the number of Z scores of the experimental drug value from the respective control
631 mean. Scores highlighted in red denote a shift towards a more proliferative
632 phenotype and scores highlighted in green denote a shift to a more senescent
633 phenotype.
634 C) P22 HMFs stained with DAPI (blue) and Cell Mask, p21, p16, IL-6, or nucleolin
635 (red), or SA-β-Gal (blue) following 96-day treatment with 5nM Rapamycin, 10nM
636 Dactolisib/BEZ235, 0.1nM Trametinib or their respective controls. Size bar,
637 100μm.

638
639 **Figure 4.** Drugs that decelerate CellAge extend lifespan *in vivo*.
640 A) Lifespan analysis on w^{Dah} background wild type flies fed with SYA food containing
641 different concentration of rapamycin or ethanol as solvent control. For each
642 condition, 150 flies were used.
643 B) Lifespan analysis on w^{Dah} background wild type flies fed with SYA food containing
644 different concentration of Dactolisib/BEZ235 or DMSO as solvent control. For each
645 condition, 150 flies were used.

646 C) Lifespan analysis on w^{Dah} background wild type flies fed with SYA food containing
647 different concentration of torin2 or DMSO as solvent control. For each condition,
648 150 flies were used.
649
650

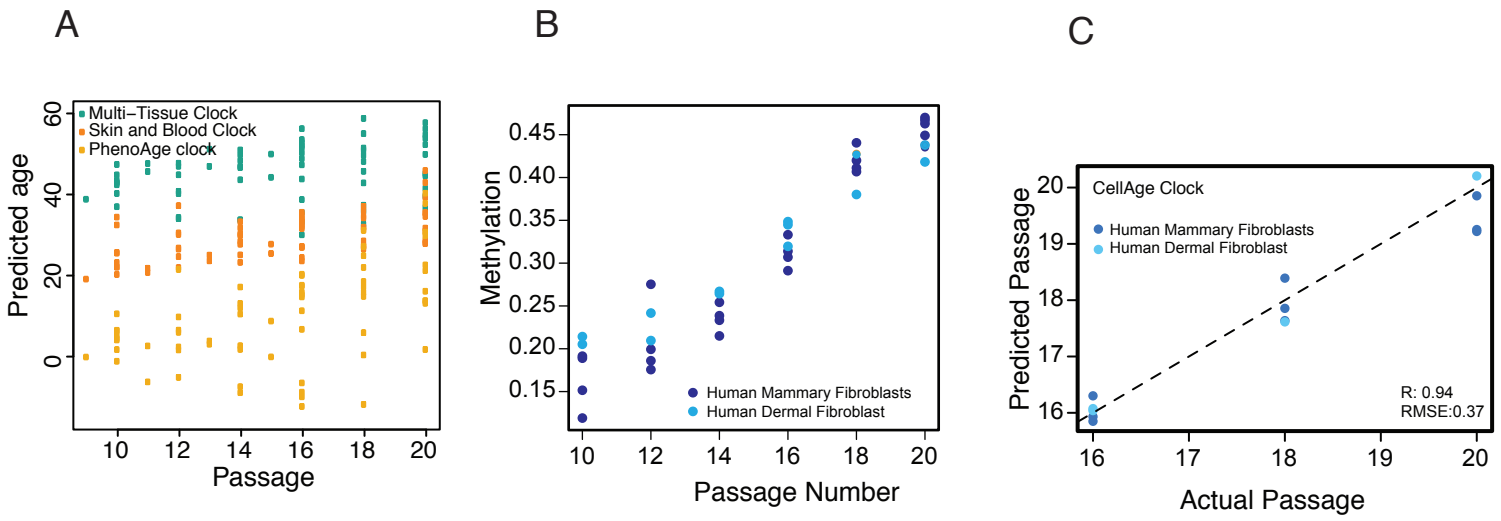
A
Multi−Tissue Clock
Skin and Blood Clock
PhenoAge clock
Predicted age
Passage
B
Methylation
Human Mammary Fibroblasts
Human Dermal Fibroblast
Passage Number
C
CellAge Clock
Human Mammary Fibroblasts
Human Dermal Fibroblast
R: 0.94
RMSE:0.37
Predicted Passage
Actual Passage

Figure 1.

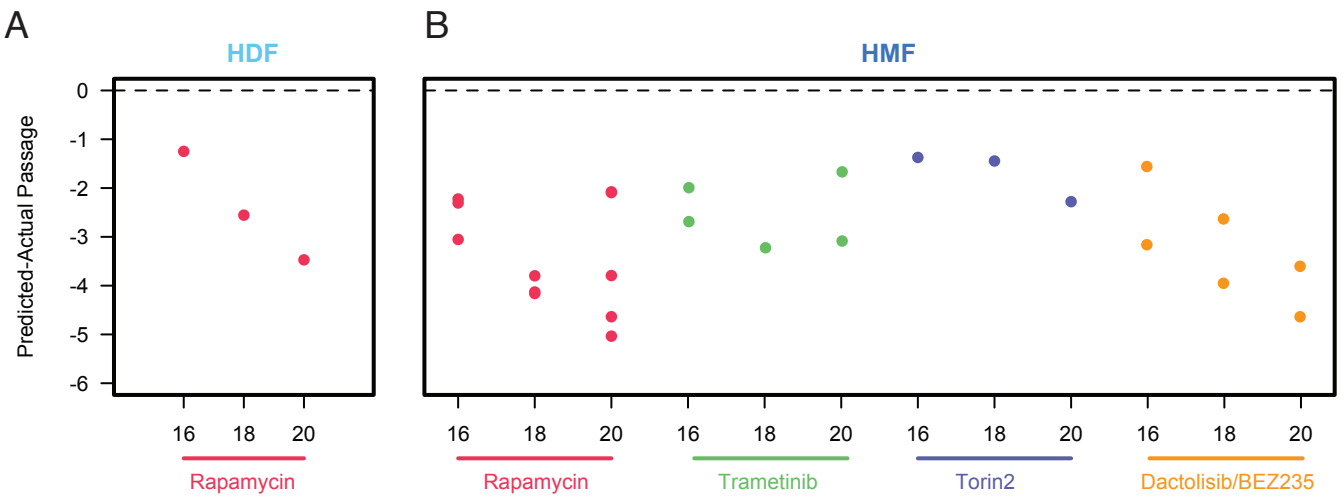
A
HDF
B
HMF
Predicted-Actual Passage
0
-1
-2
-3
-4
-5
-6
16
18
20
Rapamycin
Rapamycin
Trametinib
Torin2
Dactolisib/BEZ235

Figure 2.

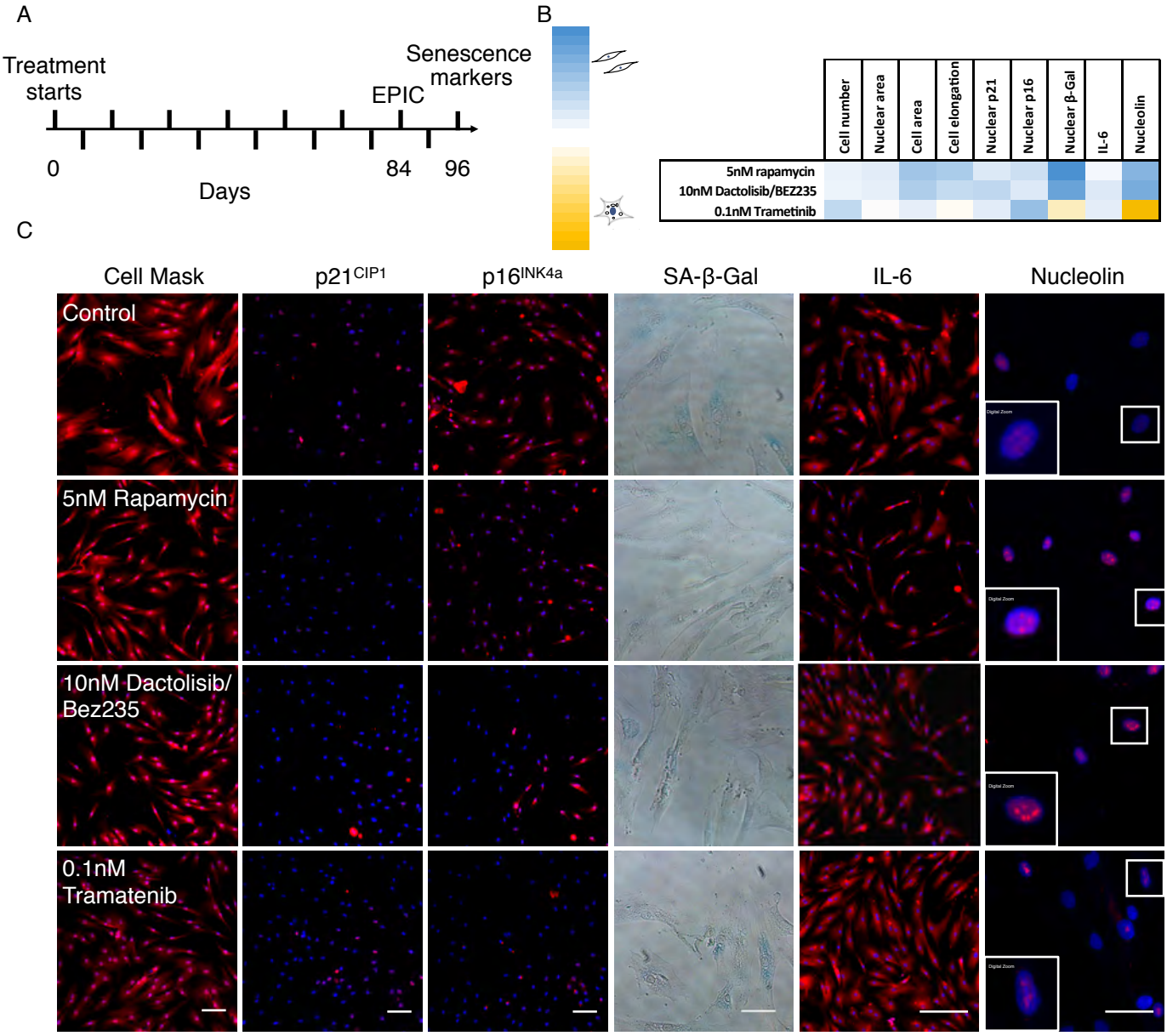
A
Treatment starts
Senescence markers
EPIC
0
84
96
Days
B
Cell number
Nuclear area
Cell area
Cell elongation
Nuclear p21
Nuclear p16
Nuclear β-Gal
IL-6
Nucleolin
5nM rapamycin
10nM Dactolisib/BEZ235
0.1nM Trametinib
C
Cell Mask
p21CIP1
p16INK4a
SA-β-Gal
IL-6
Nucleolin
Control
5nM Rapamycin
10nM Dactolisib/ Bez235
0.1nM Tramatenib

Figure 3

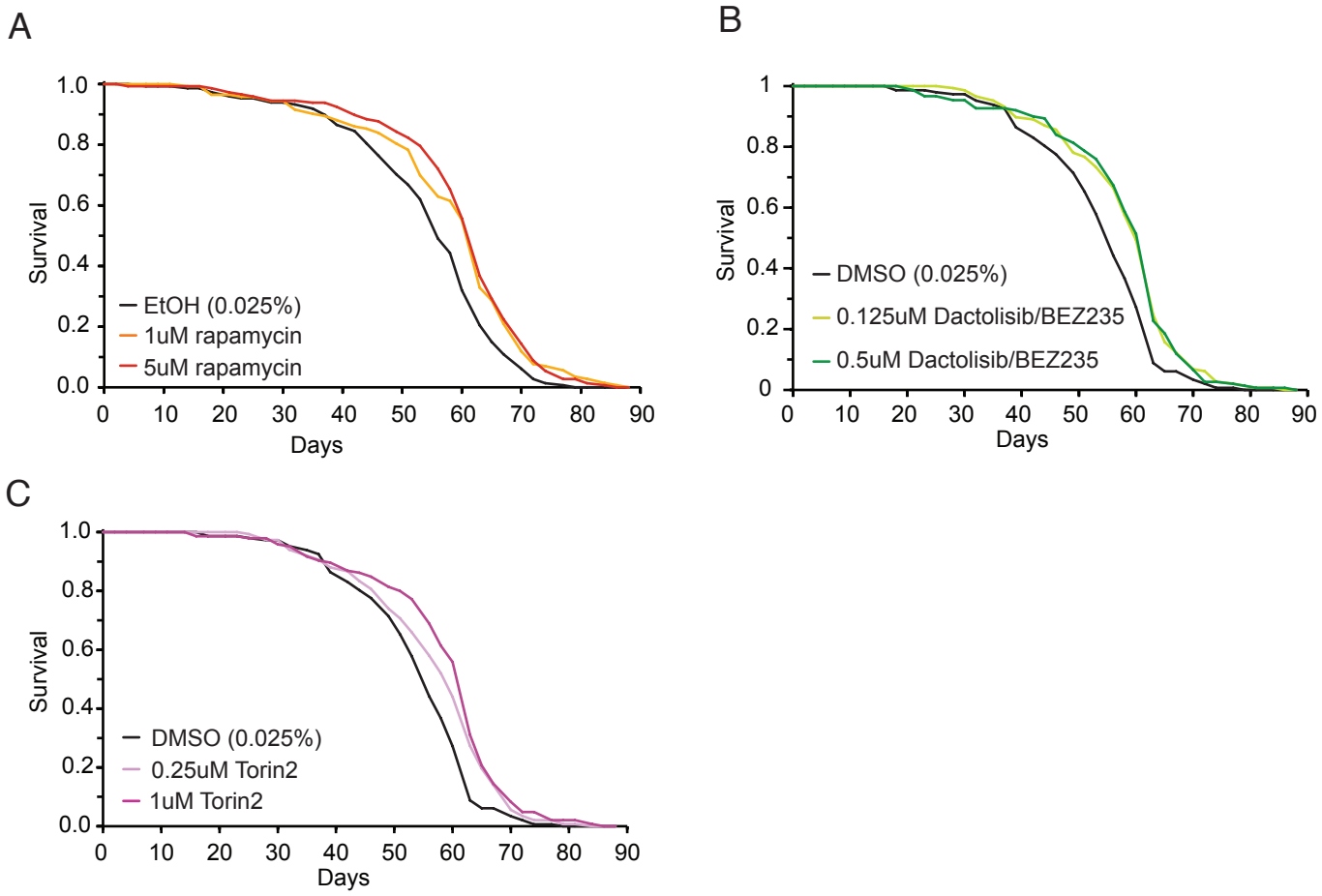
A
Survival
Days
EtOH (0.025%)
1uM rapamycin
5uM rapamycin
B
Survival
Days
DMSO (0.025%)
0.125uM Dactolisib/BEZ235
0.5uM Dactolisib/BEZ235
C
Survival
Days
DMSO (0.025%)
0.25uM Torin2
1uM Torin2

Figure 4